Chemical Science

EDGE ARTICLE

View Article Online
View Journal | View Issue

Cite this: *Chem. Sci.*, 2019, **10**, 8850

All publication charges for this article have been paid for by the Royal Society of Chemistry

Benchmark selectivity *p*-xylene separation by a non-porous molecular solid through liquid or vapor extraction†

Na Sun,[a] Shi-Qiang Wang,[c] Ruqiang Zou,[a] Wen-Gang Cui,[b] Anqi Zhang,[a] Tianzhen Zhang,[a] Qi Li,[b] Zhan-Zhong Zhuang,[a] Ying-Hui Zhang,[b] Jialiang Xu,*[b] Michael J. Zaworotko[c] and Xian-He Bu*[ab]

Received 29th May 2019
Accepted 29th July 2019

DOI: 10.1039/c9sc02621e

rsc.li/chemical-science

Solid–liquid separation of similarly sized organic molecules utilizing sorbents offers the potential for new energy-efficient approaches to a number of important industrial separations such as xylenes (C8) separations. Research on selective C8 sorption has tended to focus upon rigid porous materials such as zeolites and MOFs but has revealed generally weak selectivity that is inconsistent across the range of C8 molecules. Nevertheless, there are a few recent examples of non-porous molecular materials that exhibit relatively high selectivity for *p*-xylene (*p*X) from *p*X/*o*X, approaching that of the current benchmark *p*X sorbent, the zeolite H/ZSM-5. Herein, we report that a L-shaped Ag(I) complex, AgLClO_4 (**M**), which crystallizes as a non-porous molecular solid material, offering exceptional performance for *p*X selectivity across the range of C8 isomers with liquid extraction selectivity values of 24.0, 10.4 and 6.2 *vs.* *o*X, *e*B and *m*X, respectively. The *p*X selectivities over *o*X and *e*B are among the highest yet reported. Moreover, **M** also exhibits strong vapor extraction selectivity and can be regenerated by exposure to vacuum drying.

Introduction

Molecular separations are important in the production of clean water, specialty chemicals, commodities, and fuels.[1,2] Separation of the C8 isomers (*para*-xylene, *p*X, *ortho*-xylene, *o*X, *meta*-xylene, *m*X, ethylbenzene, *e*B) is critical as their end use includes polymers, plastics, resins, pigments, and fungicides.[3–5] Indeed, separation of xylene isomers has been described as "one of the seven chemical separations to change the world"[6] because of (i) the commercial value; and (ii) its difficulty due to their inherently similar structures and physical properties (boiling points, kinetic diameters, *etc.*, Table S1†).[7–11] Approaches such as fractional crystallization,[12] adsorption,[13] sieving,[14] complexation,[15] and isomerization[16] have been employed to separate xylene isomers. With respect to adsorption, there is of great potential to reduce the energy footprint of C8 separations, but most sorbents exhibit low selectivity for the aforementioned reasons (Table S2†). With respect to the current benchmark sorbents, it is interesting to note that, whereas rigid 3D porous materials such as MOFs are the most widely studied, they are not prominent amongst the leading materials for performance in terms of *p*X or *o*X selectivity. For example, the 0D non-porous coordination complex $[Ni(NCS)_2(ppp)_4]$[17] and the 2D layered coordination network sql-1-Co-NCS[18] are the most selective sorbents for *o*X. The leading *p*X favoring sorbents are the 0D organic molecular EtP6 [19] and the zeolite H/ZSM-5.[13]

Whereas it is perhaps counter-intuitive to study non-porous molecular solids for gas and vapor separations, their performance to date for xylenes prompted us to study other classes of molecular solids that can form host–guest complexes or inclusion compounds upon contact with organic molecules.[20] Such stimulus-induced phase transformations of host molecules has been exemplified in studies reported by the Atwood and Barbour groups.[17,21] Recently, Huang *et al.* have developed a family of nonporous adaptive crystals, which exhibited superior performances for molecular adsorption and separation.[22,23] With respect to C8 separations, Báthori,[24] Kawahata,[12] Zhang & Moore[25] and Nassimbeni[26] all demonstrated the potential for C8 isomer separation by "0D" molecular solids is promising. The nonporous adaptive crystals have been also demonstrated to be an ideal separation platform for C8 compounds.[19,27,28] These contributions prompted us to investigate a very different class of nonporous adaptive crystals based on metal–organic coordination compounds, as detailed herein.

[a]*State Key Laboratory of Elemento-Organic Chemistry, College of Chemistry, Nankai University, Tianjin 300071, China. E-mail: buxh@nankai.edu.cn*

[b]*School of Materials Science and Engineering, National Institute for Advanced Materials, TKL of Metal and Molecule-Based Material Chemistry, Nankai University, Tianjin 300350, China. E-mail: jialiang.xu@nankai.edu.cn*

[c]*Department of Chemical Sciences and Bernal Institute, University of Limerick, Limerick, Republic of Ireland*

† Electronic supplementary information (ESI) available. CCDC 1889509–1889512. For ESI and crystallographic data in CIF or other electronic format see DOI: 10.1039/c9sc02621e

Results

The non-porous molecular complex **M** was synthesized by solvothermal reaction of $AgClO_4$ with the ligand 2,3-bis[3-(pyridin-2-yl)-1*H*-pyrazol-1-yl·methyl]quinoxaline[29,30] (see full details in ESI†). **M** offers π binding sites that are readily accessible thanks to its L-shaped geometry (Fig. S1†). As we report herein, although **M** forms a non-porous molecular crystal, it switches to C8 loaded phases when exposed to C8 isomers and readily reverts to **M** upon exposure to vacuum drying (Fig. 1). Single crystals of **M** were obtained from water/methanol under solvothermal conditions. Single crystal X-ray diffraction (SCXRD) results reveal that the Ag^+ cations adopt a slightly distorted square planar coordination mode to four nitrogen atoms of two 3-(2-pyridyl)pyrazole species. The L-shaped cations feature strong C–H···π (2.79 Å and 3.32 Å) and C–H···N (2.69 Å) interactions (Fig. S1†), and form into a non-porous framework as indicated by Platon calculations (~2.6%).[31]

Solvothermal reactions in the presence of each of the pure xylene isomers (ESI, Experimental section†) afforded crystals of the respective inclusion compounds with varying host : guest ratios, *n*, for *p*X ($n = 4:5$), *m*X ($n = 2:1$) and *o*X ($n = 1:1$) (Fig. 2, S2–S8 and Table S3†). The corresponding reaction with *e*B under the same conditions did not result in an inclusion compound. The crystal structures reveal that the formation of the inclusion compounds is driven by the rearrangement of **M**, two L-shaped building blocks, into a supramolecular box-like cage. This cage enclathrates the respective guests with one xylene molecule per cage. The cage dimensions are independent of the guest: 10.28 × 7.03 × 10.07 $Å^3$ for *p*X; 10.18 × 6.98 × 10.04 $Å^3$ for *m*X; 10.26 × 7.06 × 10.02 $Å^3$ for *o*X. However, the interstitial spaces formed between the cages are different (*p*X: 3.43, 3.61 Å; *m*X: 3.47, 3.06 Å; *o*X: 4.65, 3.55 Å). It is the chemical environments between the cages that result in different host : guest ratios. For *p*X@**M**, there are four *p*X chemical environments. Two of them are inside the cage: one with ordered *p*X and the other with disordered *p*X. The other *p*X molecules lie between cages: one located between adjacent cages and the other lying in the gap of cages. For *m*X@**M**, all *m*X molecules lie in the center of cages and there are none out of the cages. For *o*X@**M**, one *o*X is inside the cage and the other lies between the cages (Fig. S3–S8†).

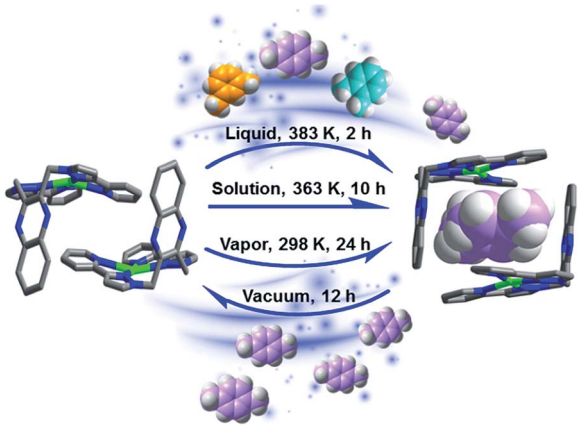

Fig. 1 Schematic illustration of the adsorption behavior of the non-porous molecular crystal **M**. **M** readily forms host–guest complexes upon exposure to xylene isomers in liquid, vapor or solution phases and can be recovered upon exposure to vacuum drying.

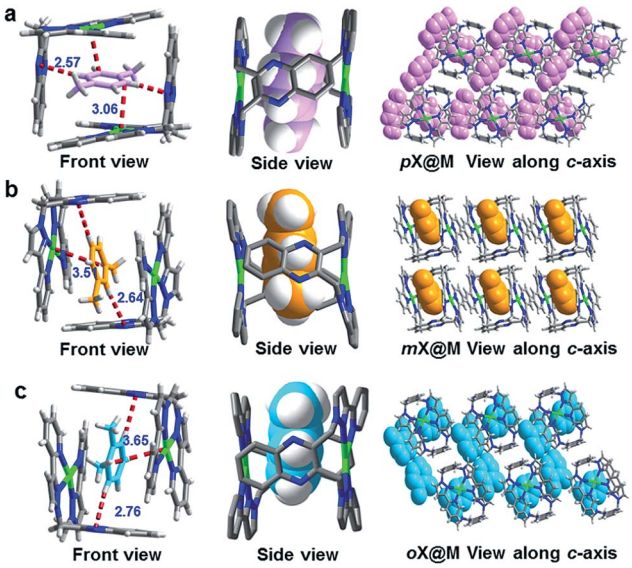

Fig. 2 Single crystal structures of the host–guest complexes formed between **M** and (a) *p*X, (b) *o*X and (c) *m*X.

Xylene selectivity studies in liquid

To study the xylene selectivity of **M**, solid–liquid sorption experiments using a 1 : 1 : 1 volumetric ratio of *o*X : *m*X : *p*X were conducted using various conditions (the solubility of the host in xylenes is negligible, Fig. S9†). Because of slow kinetics, a solvothermal method (Experimental section in ESI†) was ultimately preferred. The resulting material, *p*X/*m*X/*o*X@**M**, afforded a PXRD pattern resembling the calculated PXRD pattern of *p*X@**M** (Fig. 3a). ^{1}H NMR measurements revealed that *p*X was the predominant isomer included in *p*X/*m*X/*o*X@**M** (Fig. 3b and Table S4, ESI†).

The kinetics of solid–liquid sorption for **M** in a 1 : 1 mixture of *p*X and *o*X at 383 K was monitored by gas chromatography (GC) (Table S5†). As shown in Fig. 3c, the uptake of *p*X in **M** increased over time and after 2 h the mass percentage of *p*X reached ~12.3% *vs.* ~0.35% for *o*X. This result indicated a high selectivity of **M** towards *p*X (about 30 : 1 for *p*X & *o*X). Based upon this kinetic study, we conducted five replicates of this experiment (2 h at 383 K), and the average *p*X/*o*X selectivity was found to be 24.0. GC was then used to quantitatively determine the selectivity of **M** towards other pairs of xylene isomers following the same procedure used for *p*X/*o*X. Selectivity values of 24.0, 6.19, 10.36 and 3.93 were determined for *p*X/*o*X, *p*X/*m*X, *p*X/*e*B and *m*X/*o*X, respectively (Fig. S10–S13, Tables S6 and S7†). The *p*X/*o*X, *p*X/*e*B, *m*X/*o*X and *p*X/*m*X selectivity values demonstrated herein are among the highest values yet reported.[32–37]

Commercial grade xylenes are usually produced by methylation of toluene and benzene and contains *p*X, *m*X, *o*X and

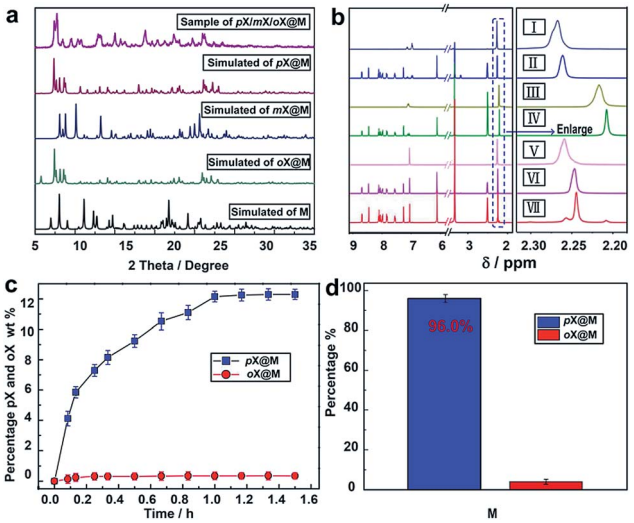

Fig. 3 Separation performance of **M** towards xylenes. (a) The PXRD pattern of *p*X/*m*X/*o*X@**M** *vs.* the calculated PXRD patterns of *o*X@**M**, *m*X@**M**, *p*X@**M**. (b) The ^{1}H NMR spectra (DMSO) of **M** after soaking in xylenes *vs.* reference extractions. *p*X is the predominant isomer: (I) *m*X; (II) *m*X@**M**; (III) *o*X; (IV) *o*X@**M**; (V) *p*X; (VI) *p*X@**M**; (VII) xylenes@**M**. (c) Kinetics of sorption for *p*X/*o*X at 383 K as determined by GC. (d) Relative amount of *p*X and *o*X extracted by **M** as measured by GC (average value of five extractions).

ethylbenzene (*e*B).[1] A commercial grade xylenes C8 mixture (*o*X : *m*X : *p*X : *e*B = 20 : 20 : 20 : 40, v/v) was also tested using the same procedure. The results suggest that **M** strongly favors *p*X over the other C8 isomers with selectivity values consistent with those obtained from the 1 : 1 extractions (Fig. S14, ESI†).

To study the recyclability of **M**, we conducted variable temperature X-ray diffraction (VT-XRD) and thermogravimetric analysis (TGA) experiments. The TGA suggest the materials

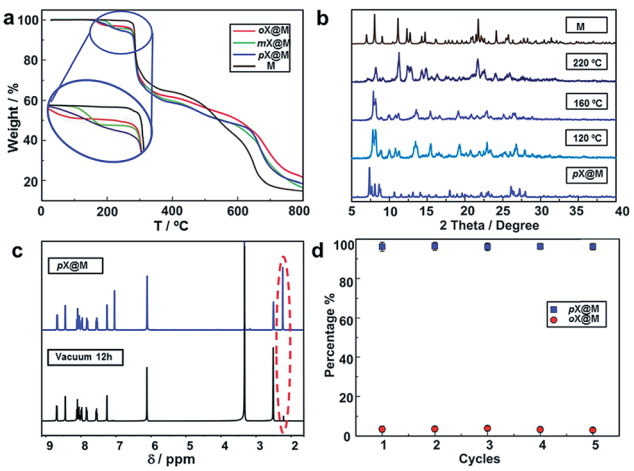

Fig. 4 Recyclability of **M**. (a) The TGA profiles for **M**, *o*X@**M**, *m*X@**M**, *p*X@**M**. Loss of weight: *p*X@**M** > *m*X@**M** > *o*X@**M**. (b) VT-XRD experiments for *p*X@**M**. With the temperature increasing, the pattern of PXRD transformed from *p*X@**M** into **M**. (c) The ^{1}H NMR spectra of *p*X@**M** and the sample after vacuum drying. (d) Relative uptake of *p*X and *o*X in **M** after **M** is recycled for 5 times.

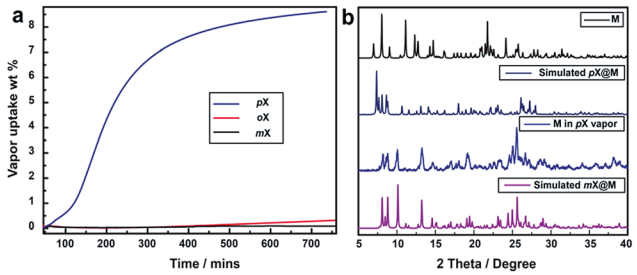

Fig. 5 Vapor sorption of **M**. (a) Kinetics of *p*X (blue), *m*X (black), *o*X (red) vapour sorption for **M** at 298 K, respectively. (b) The PXRD of **M** in *p*X vapor sorption sample is most consistent with the *m*X@**M** in liquid.

thermal stability until 573 K (Fig. 4a). The VT-XRD data suggest that increasing temperature causes *p*X@**M** to gradually transform back to **M** (Fig. 4b). ^{1}H NMR experiments were conducted after vacuum drying (Experimental section in ESI†) of a sample of *p*X@**M** for 12 h and verified the presence of **M** (Fig. 4c). Recycled samples of **M** can be used for *p*X selection experiments at least 5 times without any performance decrease (Fig. 4d).

Xylene selectivity studies in vapor

Vapor sorption experiments were conducted to determine if C8 vapors can also induce switching from closed to open phases. The kinetics of xylene vapour sorption on **M** was studied at 298 K (Fig. 5a). It reveals that, under the same conditions, *p*X vapor can be adsorbed much more efficiently and sufficiently than *m*X or *o*X. This could be attributed to the smaller kinetic diameter of *p*X (Table S1†), which benefits the diffusion of *p*X in the structure of **M** for faster occupation of the "box-like" cage. It was observed that, whereas **M** switches in the presence of *p*X vapor, there are differences in terms of uptake and structure *vs.* the solution experiments. As shown in Fig. 5b, the PXRD of **M** after *p*X vapor sorption sample is consistent with that of **M** after contact with *m*X solution. The mass uptake and PXRD are consistent with $n = 2:1$ and *p*X molecules can be removed *in vacuo* drying to regenerate **M** (Fig. S15†).

Vapour-phase binary mixture separation experiments were conducted on **M** and selectivities were determined by GC. Selectivity values were found to be 20.3, 5.4, 8.0 and 1.15 for *p*X/*o*X, *p*X/*m*X, *p*X/*e*B and *m*X/*o*X, respectively (Fig. S16–S20, Tables S8 and S9†). The hierarchy of the selectivity (*p*X > *m*X > *o*X) is consistent with that observed during the liquid sorption experiments. The *p*X/*o*X selectivity of 20.3 is to our knowledge among the highest value yet reported for vapor extractions (Table S2†).

Discussion

To understand the mechanism behind the observed selectivity of **M** for *p*X, we analyzed the crystal structures with particular emphasis upon host–guest interactions. For guests within the cage (Fig. 2 and S3–S8†), the shortest distance between *p*X molecules and **M** results from C–H···N interactions formed by aromatic C–H moieties and the quinoxaline rings. This distance

is shortest for *p*X: 2.57 *vs.* 2.64 *vs.* 2.76 Å for *p*X, *m*X and *o*X, respectively. The interaction distances between the benzene ring of each xylene and Ag^+ cations in the coordination complex are also shortest for *p*X (3.06 *vs.* 3.51 *vs.* 3.65 Å for *p*X, *m*X and *o*X, respectively). These differences in host–guest interactions can be attributed to shape differences of the C8 aromatics with *p*X enabling closer interactions, presumably because the methyl groups can orient towards the windows of the cage. This could be helps to explain why **M** exhibits high *p*X selectivity (Table S2†). Moreover, DFT calculations also proved that the binding energy of *p*X@**M** is higher than that of *o*X@**M** and *m*X@**M** (Table S10†). This is in consistent with the kinetics studies (Fig. 3c and 5a) and could be the reason why **M** has a high selectivity for *p*X.

We note that, because **M** forms a distinct cage-like structure that serves as a host for xylenes, it exhibits a different binding phenomenon from that observed in other molecular compounds that exhibit such high selectivity, EtP6 (ref. 19) (*p*X selective) and $[Ni(NCS)_2(ppp)_4]$[17] (*o*X selective, Table S2†). Further, the shape of the supramolecular cage formed by **M** enables us to gain insight into the selectivities observed herein, which for *p*X/*o*X and *p*X/*e*B are among the highest yet reported. The behavior observed herein is therefore most closely related to clathration approaches driven by weak van der Waals interactions reported by Atwood and Barbour *et al.*[21]

Conclusion

In summary, the L-shaped non-porous molecular material **M** exhibits new benchmarks for *p*X selectivity as it preferentially forms host–guest complexes with *p*X from liquid or vapor C8 mixtures. We attribute the performance of **M** to its ability to form a cage-like structure that is well-suited for the size and shape of *p*X. Although the approach taken herein, the use of a non-porous solid to serve as a selective sorbent, is perhaps counter-intuitive, it offers superior performance *vs.* rigid porous materials such as zeolites and MOFs. Moreover, as is likely to be the case for molecular materials in general, **M** is readily recyclable. Whereas the promise for non-porous molecular materials to serve as selective sorbents is high based upon this and other recent studies, slow kinetics and low uptake remain unsolved challenges for molecular materials. Future work will focus upon overcoming such problems.

Conflicts of interest

The authors declare no competing financial interest.

Acknowledgements

This work was financially supported by the National Natural Science Foundation of China (91256124, 21531005 and 21773168) and "111 Project" of China (B18030). We also gratefully acknowledge the support of Science Foundation Ireland (13/RP/B3529 and 16/IA/4624).

Notes and references

1 J. Fabri, U. Graeser and T. A. Simo, *Ullmann's Encyclopedia of Industrial Chemistry*, Wiley-VCH, Weinheim, Germany, 2000.
2 Materials for Separation Technologies, *Energy and Emission Reduction Opportunities*, Oak Ridge National Laboratory, Oak Ridge, TN, USA, 2005.
3 M. Minceva and A. E. Rodrigues, *AIChE J.*, 2007, **53**, 138.
4 J. Scheirs and T. E. Long, *Industrial Modern Polyesters: chemistry and technology of polyesters and copolyesters*, Wiley, Chichester, 2003.
5 J. L. Pellegrino, *Energy and Environmental Profile of the Chemicals Industry*, U.S. Department of Energy, 2000.
6 D. S. Sholl and R. P. Lively, *Nature*, 2016, **532**, 435.
7 R. Krishna, *Phys. Chem. Chem. Phys.*, 2015, **17**, 39.
8 D. Peralta, G. Chaplais, J.-L. Paillaud, A. Simon-Masseron, K. Barthelet and G. D. Pirngruber, *Microporous Mesoporous Mater.*, 2013, **173**, 1.
9 A. Méthivier, in *Zeolites for Cleaner Technologies, Catalytic Science Series*, Imperial College Press, London, 2002, vol. 3, pp. 209–221.
10 R. Szostak, *Handbook of Molecular Sieves: Structure*, Springer, 1992.
11 P. S. Barcia, D. Guimaraes, P. A. P. Mendes, J. A. C. Silva, V. Guillerm, H. Chevreau, C. Serre and A. E. Rodrigues, *Microporous Mesoporous Mater.*, 2011, **139**, 67.
12 M. Kawahata, T. Hyodo, M. Tominaga and K. Yamaguchi, *CrystEngComm*, 2018, **20**, 5667.
13 M. Rasouli, N. Yaghobi, S. Chitsazan and M. H. Sayyar, *Microporous Mesoporous Mater.*, 2012, **150**, 47.
14 D.-Y. Koh, B. A. McCool, H. W. Deckman and R. P. Lively, *Science*, 2016, **353**, 804.
15 W.-Y. Zhang, Y.-J. Lin, Y.-F. Han and G.-X. Jin, *J. Am. Chem. Soc.*, 2016, **138**, 10700.
16 J. Jarvis, P. He, A. Wang and H. Song, *Fuel*, 2019, **236**, 1301.
17 M. Lusi and L. J. Barbour, *Angew. Chem., Int. Ed.*, 2012, **51**, 3928.
18 S.-Q. Wang, S. Mukherjee, E. Patyk-Kazmierczak, S. Darwish, A. Bajpai, Q.-Y. Yang and M. J. Zaworotko, *Angew. Chem., Int. Ed.*, 2019, **58**, 6630.
19 K. Jie, M. Liu, Y. Zhou, M. A. Little, A. Pulido, S. Y. Chong, A. Stephenson, A. R. Hughes, F. Sakakibara, T. Ogoshi, F. Blanc, G. M. Day, F. Huang and A. I. Cooper, *J. Am. Chem. Soc.*, 2018, **140**, 6921.
20 H.-N. Zhang, Y. Lu, W.-X. Gao, Y.-J. Lin and G.-X. Jin, *Chem.–Eur. J.*, 2018, **24**, 18913.
21 J. L. Atwood, L. J. Barbour, A. Jerga and B. L. Schottel, *Science*, 2002, **298**, 1000.
22 K. C. Jie, Y. J. Zhou, E. R. Li, Z. T. Li, R. Zhao and F. H. Huang, *J. Am. Chem. Soc.*, 2017, **139**, 15320.
23 K. C. Jie, Y. J. Zhou, E. R. Li and F. H. Huang, *Acc. Chem. Res.*, 2018, **51**, 2064.
24 M. M. Wicht, L. R. Nassimbeni and N. B. Báthori, *Polyhedron*, 2019, **163**, 7.
25 D. Venkataraman, S. Lee, J. Zhang and J. S. Moore, *Nature*, 1994, **371**, 591.

26 L. R. Nassimbeni, *Acc. Chem. Res.*, 2003, **36**, 631.
27 K. C. Jie, M. Liu, Y. J. Zhou, M. A. Little, S. Bonakala, S. Y. Chong, A. Stephenson, L. J. Chen, F. H. Huang and A. I. Cooper, *J. Am. Chem. Soc.*, 2017, **139**, 2908.
28 B. Gao, L. L. Tan, N. Song, K. Li and Y. W. Yang, *Chem. Commun.*, 2016, **52**, 5804.
29 R.-Q. Zou, C.-S. Liu, Z. Huang, T.-L. Hu and X.-H. Bu, *Cryst. Growth Des.*, 2006, **6**, 99.
30 F. Li, J. K. Clegg, L. Goux-Capes, G. Chastanet, D. M. D'Alessandro, J.-F. Letard and C. J. Kepert, *Angew. Chem., Int. Ed.*, 2011, **50**, 2820.
31 A. L. Spek, *Acta Crystallogr., Sect. C: Struct. Chem.*, 2015, **71**, 9.
32 Z.-Y. Gu, D.-Q. Jiang, H.-F. Wang, X.-Y. Cui and X.-P. Yan, *J. Phys. Chem. C*, 2010, **114**, 311.
33 J.-M. Lin, C.-T. He, P.-Q. Liao, R.-B. Lin and J.-P. Zhang, *Sci. Rep.*, 2015, **5**, 11537.
34 J. E. Warren, C. G. Perkins, K. E. Jelfs, P. Boldrin, P. A. Chater, G. J. Miller, T. D. Manning, M. E. Briggs, K. C. Stylianou, J. B. Claridge and M. J. Rosseinsky, *Angew. Chem., Int. Ed.*, 2014, **53**, 4592.
35 M. Rasouli, N. Yaghobi, F. Allahgholipour and H. Atashi, *Chem. Eng. Res. Des.*, 2014, **92**, 1192.
36 M. Rasouli, N. Yaghobi, S. Z. M. Gilani, H. Atashi and M. Rasouli, *Chin. J. Chem. Eng.*, 2015, **23**, 64.
37 F. Vermoortele, M. Maes, P. Z. Moghadam, M. J. Lennox, F. Ragon, M. Boulhout, S. Biswas, K. G. M. Laurier, I. Beurroies, R. Denoyel, M. Roeffaers, N. Stock, T. Düren, C. Serre and D. E. De Vos, *J. Am. Chem. Soc.*, 2011, **133**, 18526.